HOSTED BY
ELSEVIER
CrossMark
Available online at www.sciencedirect.com
ScienceDirect
Progress in Natural Science: Materials International 25 (2015) 327–333
Progress in Natural Science Materials International
www.elsevier.com/locate/pnsmi
www.sciencedirect.com

Original Research

Electrospun composites of PHBV/pearl powder for bone repairing

Jingjing Bai, Jiamu Dai, Guang Li*

College of Material Science and Engineering, Donghua University, Shanghai, 201620, China

Received 28 June 2015; accepted 20 July 2015
Available online 1 September 2015

Abstract

Electrospun fiber has highly structural similarity with natural bone extracelluar matrix (ECM). Many researches about fabricating organic–inorganic composite materials have been carried out in order to mimic the natural composition of bone and enhance the biocompatibility of materials. In this work, pearl powder was added to the poly (3-hydroxybutyrate-co-3-hydroxyvalerate) (PHBV) and the composite nanofiber scaffold was prepared by electrospinning. Mineralization ability of the composite scaffolds can be evaluated by analyzing hydroxyapatite (HA) formation on the surface of nanofiber scaffolds. The obtained composite nanofiber scaffolds showed an enhanced mineralization capacity due to incorporation of pearl powder. The HA formed amount of the composite scaffolds was raised as the increase of pearl powder in composite scaffolds. Therefore, the prepared PHBV/pearl composite nanofiber scaffolds would be a promising candidate as an osteoconductive composite material for bone repairing.

Keywords: Hydroxyapatite; Pearl; PHBV; Mineralization; Composite nanofibers scaffolds

1. Introduction

Bone extracelluar matrix (ECM) is a type of nanocomposite on which cells adhere, proliferate and differentiate [1]. The structure of bone ECM is organic collagenous fibers embedded by inorganic hydroxyapatite (HA) nanocrystals. Many processing techniques have been developed to mimic bone ECM. Electrospinning is a simple method to fabricate nanofiber. This electrospun fiber has highly structural similarity with natural bone ECM [2–6]. The fibrous surfaces fabricated by electrospinning can improve cell adhesion when compared with smooth surfaces [7]. Recently many synthetic polymers have been used in electrospinning, such as, poly lactic acid (PLA) [8,9], polycaprolactone (PCL) [10], and poly(3-hydroxybutyrate-co-3-hydroxyvalerate) (PHBV)[11–14].

PHBV produced by microbial fermentation is one of the biomaterials applied in bone tissue engineering. It has being researched as a substitute for natural bone because of its biodegradability and biocompatibility. The degradation time of PHBV can be controlled by adding inorganic materials in PHBV matrix such as HA [15]. Besides, the ultimate degradation product of PHBV is hydroxybutyric acid which is a constituent of human blood [16–18].

The method using inorganic materials to improve both mechanical properties and biocompatibility of synthetic ECM has attracted much attention [19–21]. Using Pearl powder to enhance biological and mechanical performances has been studied recently [22]. Pearls contain growth factors that are able to increase osteoblast proliferation [23]. Furthermore, it is approved that pearl shows great biocompatible and biodegrade ability [24].

In this study, we selected PHBV as the main matrix and pearl powder as inorganic additive. The PHBV/Pearl powder composite scaffolds were prepared by electrospinning. HA would deposit on PHBV/pearl nanofiber scaffold by mineralization method in vitro. The effects of pearl powder on the surface morphology of electrospun fibers and mineralization rate were discussed here.

*Corresponding author. Tel.: +86 6779 2830.
E-mail addresses: jingjing-bai@outlook.com (J. Bai), lig@dhu.edu.cn (G. Li).

Peer review under responsibility of Chinese Materials Research Society.

http://dx.doi.org/10.1016/j.pnsc.2015.07.004

2. Materials and methods

2.1. Materials

PHBV (PHV content: 2 wt%) and pearl powder (100 nm) were purchased from Tianan biomaterials LTD (Ningbo, China) and Fenix Pearl-biotech CO.,LTD. (Zhejiang, China), respectively. 1,1,1,3,3,3-hexafluoro-2-isopropanol (HFIP) were purchased from Darui LTD. (Shanghai China).

2.2. Pretreatment of pearl

Before added in PHBV solution, pearl powder was pretreated in polyethylene glycol (PEG) solution with the aim at raising compatibility. First, suspensions were obtained by dispersing pearl powder in deionized water by stirring, then PEG powder was added to the suspensions (mass ratio of PEG/pearl = 1/20) combing ultrasonic and stiring. Each process lasted for 1 h. The suspensions were frozen overnight, and then were freeze-dried for two days.

2.3. Production of PHBV/pearl nanofibers

Pearl powder and PHBV were used to produce composite nanofibers. First, polymer solution was obtained by dissolving PHBV in HFIP at room temperature, and then pearl powder was added to the solution with sufficient stirring. In order to examine the effect of pearl powder content on fiber morphology, the polymer solution was prepared by adding varied mass ratio of pearl/PHBV in the range of 0%, 2%, 4%, and 6%.

2.4. Mineralization ability

The osteogenetic activity of the nanofibers scaffolds were generally characterized by forming bonelike HA on its surface. The nanofiber scaffolds were soaked in 1.5 simulated body fluid (1.5 SBF) for a few days and 1.5 SBF was prepared according to the method described in reference [25]. After mineralization, the nanofibers scaffolds were washed with deionized water to remove residual salts and dried before further analysis.

2.5. Mineralized sample characterization

The morphology of nanofibers scaffolds before and after soaked in SBF were characterized by scanning electron microscopy (SEM, JSM-5600 LV, JEOL, Japan). Attenuated total reflectance-Fourier transform infrared spectroscopy (ATR-FTIR) was performed by a Nicolet-670 FTIR spectrometer (NIcolet-Thermo, USA). All spectra were measured in the wavelength range of 500–4000 cm^{-1} with a resolution of 4 cm^{-1}. X-ray diffraction (XRD) Patterns were obtained with a D/max-2500 PC diffractometer (Rigaku co., Japan) using Cu/k_α radiation with wavelength of 0.154 nm at 40 kV and 200 Ma over the range of 0–60°. The thermogravimetric analysis (TGA) was employed to evaluate the weight loss of the samples in nitrogen from room temperature to 900 °C at a heating rate of 10 °C/min using a thermal analyzer (TG 209 F1, Germany).

2.6. Cell culture

MC3T3 cells were used in this work. The cells were incubated with α-MEM medium supplemented with 10% PBS, 100 U/mL penicillin and 100 μg/mL streptomycin at 37 °C in a humidified atmosphere containing 5% CO_2. Samples were placed in 24-well dishes. Before seeding cells ($2*10^4$ per well), the samples were soaked in 75% ethanol aqueous solution for at least 1 day.

2.7. MTT assay

MTT assay was applied to evaluate the cell proliferation on samples. After incubating for a certain time, the old media was

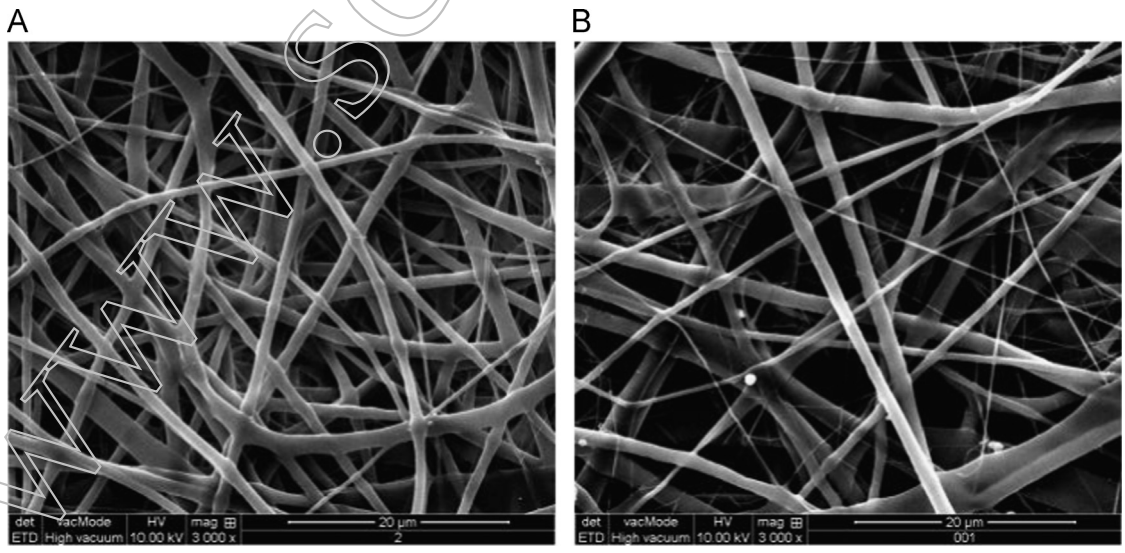

Fig. 1. SEM micrographs of electrospun fibers using PHBV solution in HFIP.(A) 4 wt% and (B) 5 wt%.

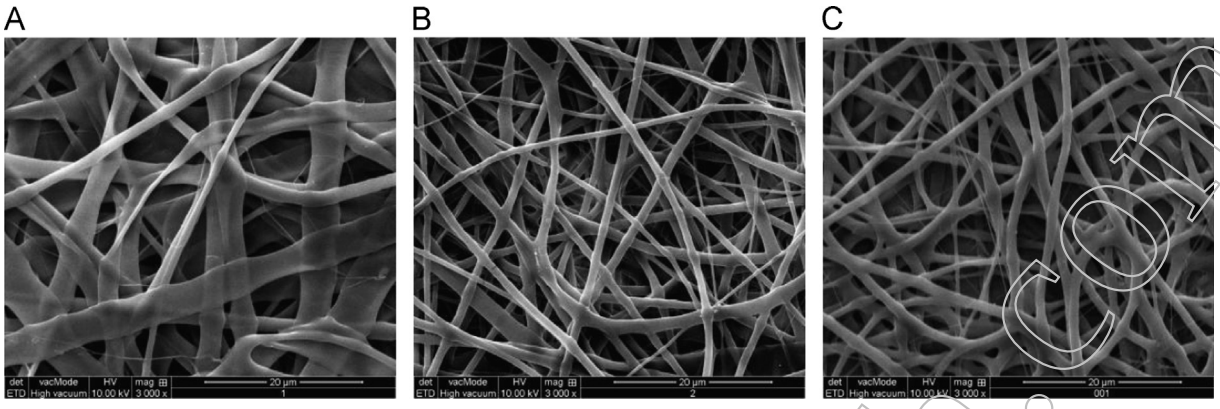

Fig. 2. SEM micrographs of electrospun fibers using different voltage.(A) 11 kV, (B) 17 kV, and (C) 22 kV.

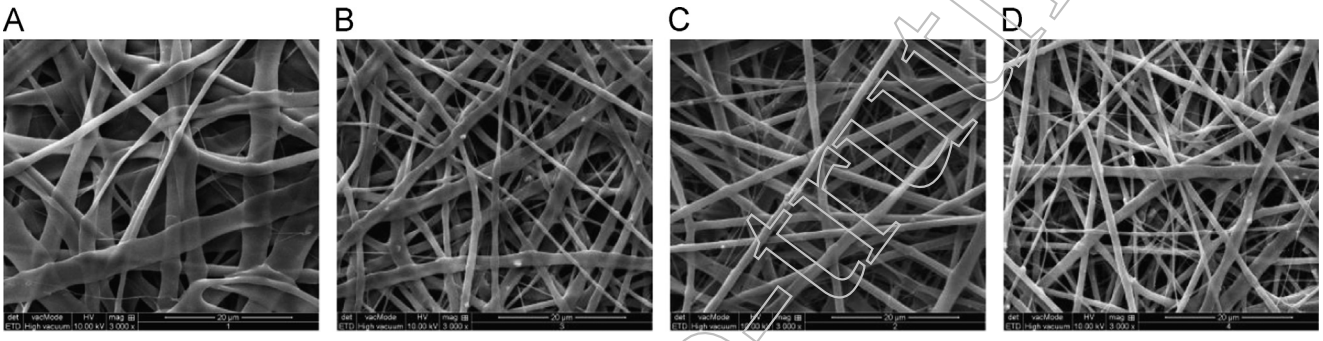

Fig. 3. SEM micrographs of electrospun fibers with different content of pearl powder using voltage of 11 kV.(A) 0 wt%, (B) 2 wt%, (C) 4 wt%, and (D) 6 wt%.

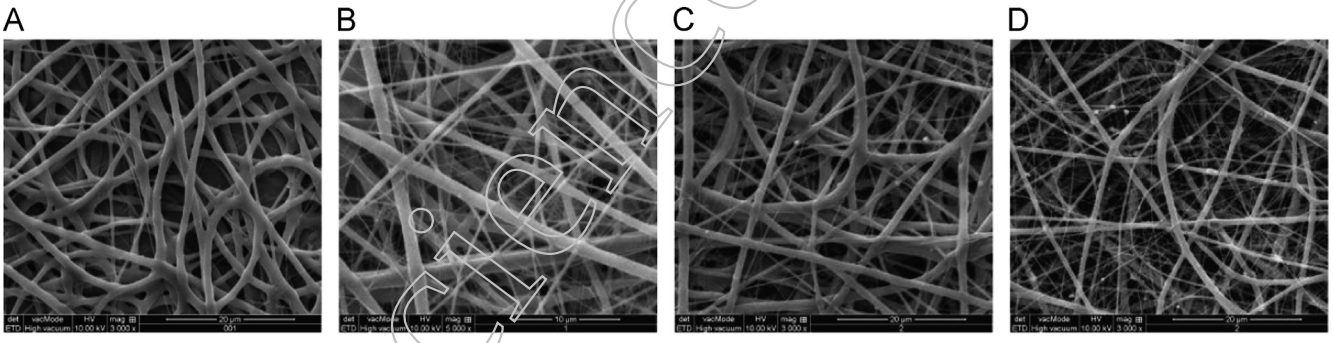

Fig. 4. SEM micrographs of electrospun fibers with different content of pearl powder using voltage of 22kV.(A) 0 wt%, (B) 2 wt%, (C) 4 wt%, and (D) 6 wt%.

removed and 360 μl new media with 40 μl MTT (5 mg/ml) solution were added in each well. The samples were incubated for 4 h. Then the solution was removed and 400 μl dimethyl-sulfoxide (DMSO) was added. Then the plate was placed in a shake for 10 min in 37 °C. The absorbance of supernatant was measured with microplate reader (MK3, thermo,USA).

2.8. Cell morphology observation

Cell morphology was evaluated by using confoeal laser scanning microscopy (CLSM). The MC3T3 cells were seeded and incubated on samples placed in 24-well dishes for 3 days. After washed with PBS and fixed with 4% glutaraldehyde for 10 min at 4 °C, samples were permeabilized in 0.1% Triton X-100 in PBS for 5 min. After washed with PBS, the fixed cells on samples were stained with Alexa Fluor@ 488

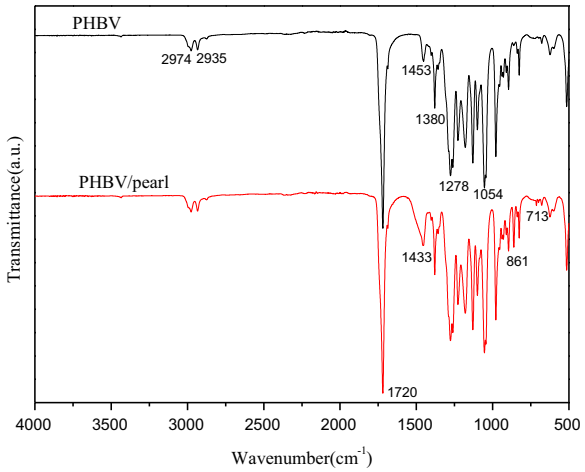

Fig. 5. ATR-FT IR spectra of PHBV and PHBV/pearl nanofiber.

phalloidin solution (165 nM) for 20 min to labeling cytoplasm, then the cells were washed again with PBS and stained with DAPI solution (100 nM) for 5 min to labeling nucleus. Then samples were washed with PBS and observed by CLSM.

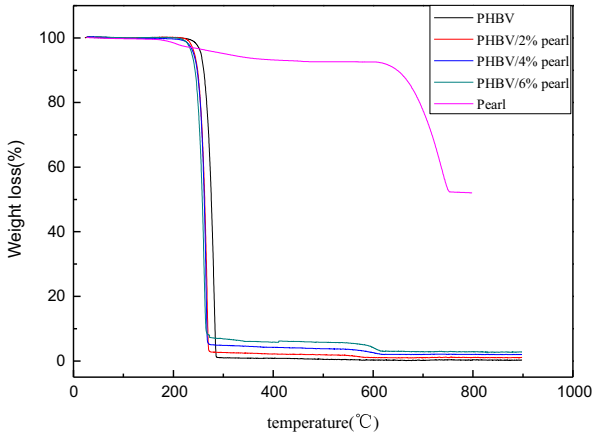

Fig. 6. TGA curves of PHBV and PHBV/pearl nanofiber.

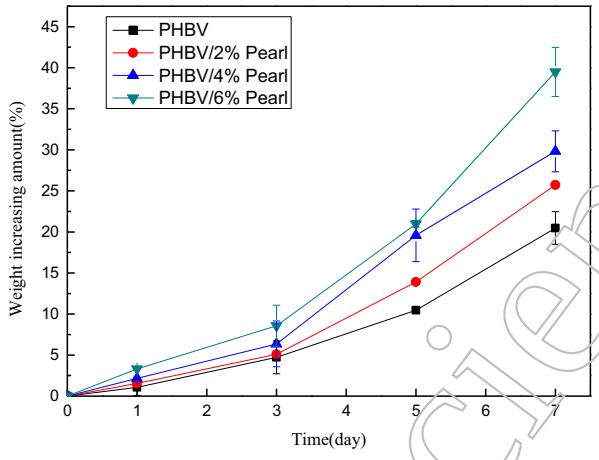

Fig. 7. Influence of pearl concentration and soaking time on HA deposition.

3. Result and discussion

3.1. Electrospinning

To evaluate the effect of concentration and voltage, the electrospinning was undertook with different concentration solutions (4, 5 wt%) and different voltage (11 kV, 17 kV, and 22 kV). The Morphology of electrospun PHBV nanofiber scaffolds prepared from different concentration solutions were shown in Fig. 1. The nanofiber resulted from 4 wt% solution showed a better morphology than that from 5 wt% and more uniform diameter distribution of fibers. Thus, the solution of 4 wt% was fixed for further experiments.

Fig. 2 showed PHBV nanofiber scaffolds fabricated on different voltage (11 kV, 17 kV, and 22 kV). The fiber diameter became smaller and more uniform with the voltage increasing, while the fiber displayed a collapsing type under low voltage.

Figs. 3 and 4 were PHBV/pearl composite nanofibers with the voltage of 11 kV and 22 kV respectively. As shown in these pictures, the addition of pearl powder improves the spinnability of the PHBV solution. The diameter of nanofibers was thinner because of the addition of pearl powder. The reason maybe that calcium carbonate in pearl powder plays a role as a lubricant, which may lead to the viscosity reduction of the blend solutions.

ATR-FTIR spectra of nanofiber were shown in Fig. 5, the C=O stretching vibration of PHBV appeared at 1720 cm^{-1}, whereas C–O stretching bands were at 1278 and 1054 cm^{-1}. C–H stretching bands were at around 2974 and 2935 cm^{-1}, besides C–H bending vibrations appeared at 1453 and 1380 cm^{-1}.The ATR-FTIR spectrum of PHBV/pearl showed absorption peaks at around 1433, 863 and 713 cm^{-1}, corresponding asymmetric stretching vibration of C–O, out-of-plane bending vibration of CO_3^{2-} and in plane bending vibration of O–C–O, respectively.

When electrospinning of organic–inorganic compounds, special attention should be paid in solution preparation since the composite solution brings about dispersion problems [26,27]. The TG analysis was used to evaluate the content of pearl powder in composite nanofibers. As shown in Fig. 6, the thermogram of PHBV nanofiber showed a one-step thermal degradation between

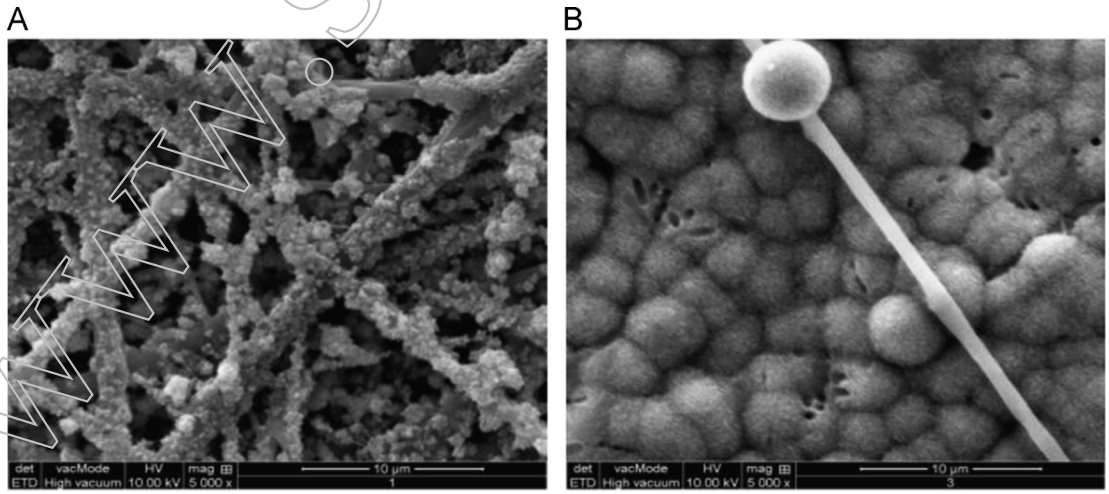

Fig. 8. SEM of HA deposited on PHBV scaffold after soaked in SBF for 3 and 7 days.

260 and 285 °C, whereas the thermogram of PHBV/ pearl nanofiber showed two steps, with the second step of degradation at about 600 °C, which can be attributed to the decomposition of pearl. Moreover, the residual mass from the present pearl powder becomes high with increasing content of pearl powder. In a summary, it was showed that the pearl powder evenly dispersed in the viscous polymer solution.

3.2. Mineralization studies

Mineralization ability of the nanofiber scaffolds can be evaluated by analyzing HA formation on the surface of nanofiber scaffolds. After soaked in 1.5SBF for a few days, the weight increasing rate of the composite nanofiber scaffolds were calculated as shown in Fig. 7. The HA deposited on the surface of pristine PHBV nanofiber scaffolds was less than that on composite nanofiber scaffolds. This indicates that pearl performed as a crystal nucleus for HA particle depositing. It has been reported that Ca^{2+} which would induce the deposition of HA particles were released from pearl powder when the PHBV/pearl nanofiber scaffolds were soaked in SBF [28]. The influence of soaking time was also showed in Fig. 7. For HA deposition, crystal nucleus is needed. However, there is no nucleus existing on PHBV nanofiber, therefore a long nucleus inducing period is acquired; then the first formed HA particles work as crystal nucleus for further mineralization. After soaked in SBF for 7 days a plenty of HA particles deposited on both PHBV and composite nanofiber scaffolds. The weight increasing amount on PHBV nanofiber scaffolds was 20%, and that is the half of the weight increasing amount on PHBV/pearl containing 6% pearl powder nanofiber scaffolds, indicating that the pearl powder enhanced the HA deposition ability.

Furthermore, the micrograph of HA particles deposited on the surface were observed in Fig. 8. after soaked for 3 days the HA particles with sphere outline generated, and after soaked

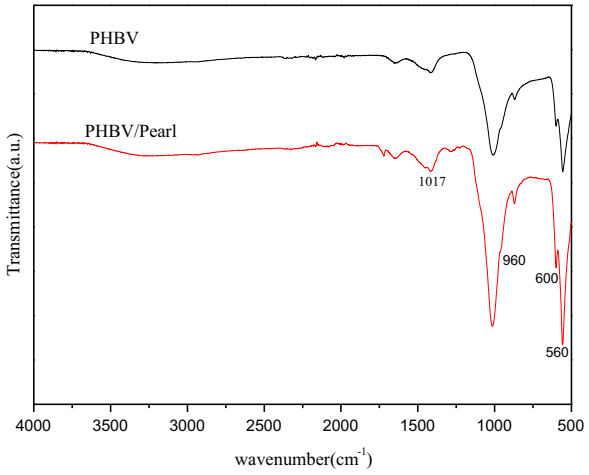

Fig. 9. ATR-FTIR spectra of PHBV and PHBV/pearl after mineralization in SBF .

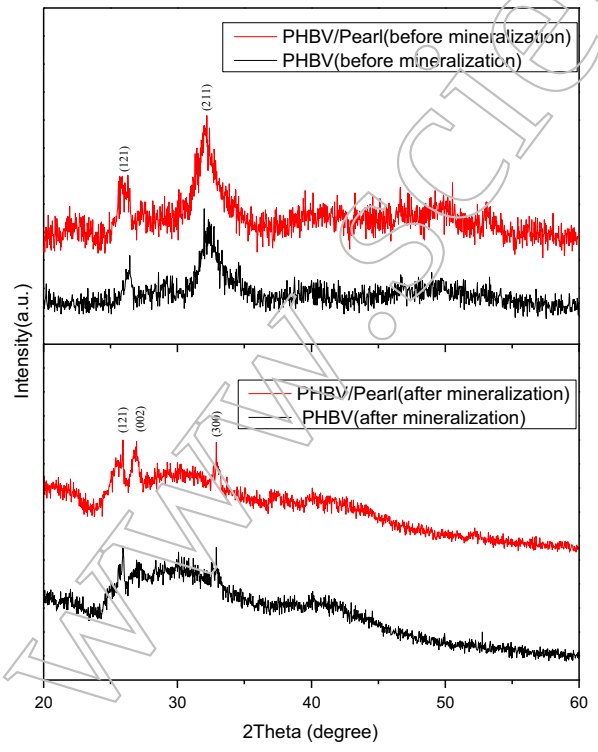

Fig. 10. XRD diffraction patterns of scaffolds before and after mineralization.

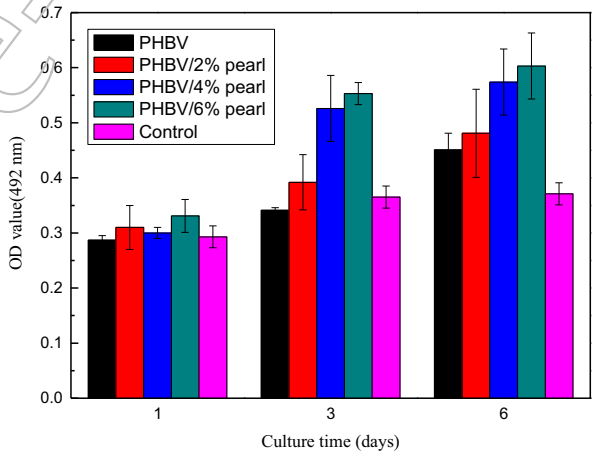

Fig. 11. Biocompatibility test of samples with and without pearl.

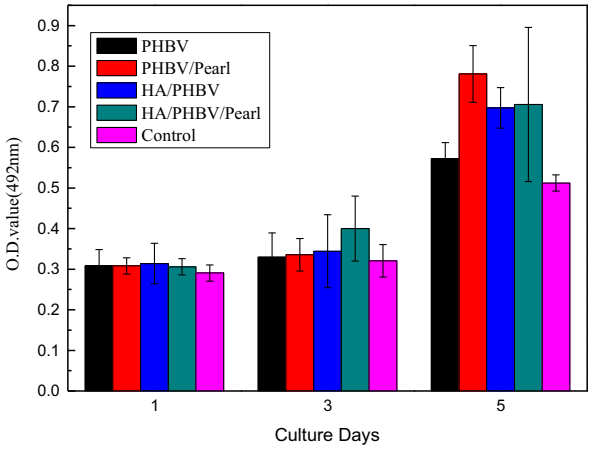

Fig. 12. Biocompatibility test of samples before and after mineralization.

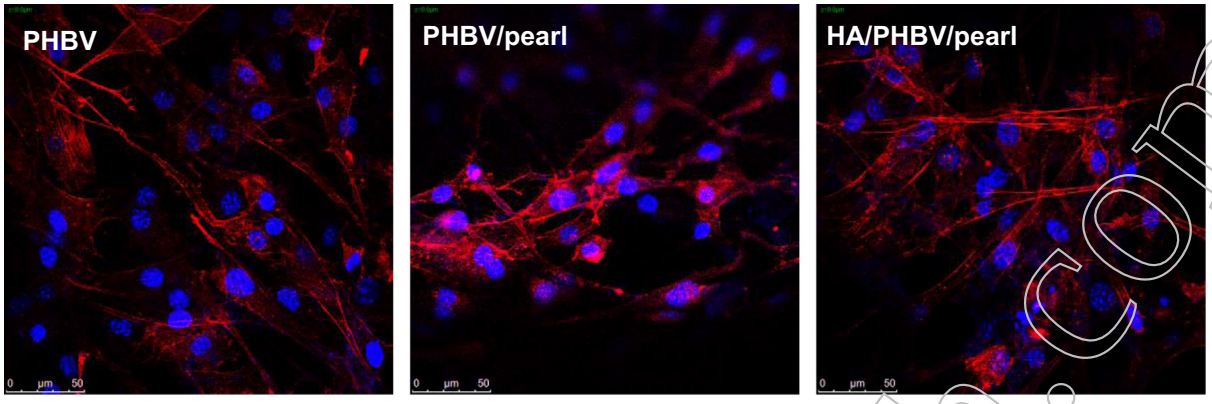

Fig. 13. Confocal microscopy of MC3T3 cells cultivated.

for 7 days, formation of HA particles were observed throughout the PHBV nanofiber scaffolds as expected.

3.3. HA structure analysis

The FTIR spectra of nanofiber scaffolds before and after mineralization showed that new peaks appeared for mineralized scaffold due to the HA particle deposition (Fig. 9). Because of the intense HA deposition on the surface, a sharp decrease of C=O and C–O stretching vibration was shown. Peaks at 1017 and 960 cm^{-1} were asymmetric and symmetric stretching vibrations of PO_4^{3-} respectively. Peaks at 600 and 560 cm^{-1} were P–O bending modes of the phosphate groups.

XRD diffraction patterns of PHBV and PHBV/pearl nanofiber scaffold before and after mineralization for 30 days were given in Fig. 10. The characteristic peaks of PHBV were at $2\theta=25.7^{\circ}$ and 31.7°. After soaked in SBF for 30 days the additional peaks related to HA appeared at $2\theta=25.9^{\circ}$ (002) and 32.9° (300), as shown in Fig. 10. In short summary, the deposited HA on the surface of different nanofiber scaffolds were almost the same both in constitution and structure.

3.4. Biocompatibility analysis

To verify cell proliferation improvement of the PHBV/pearl, MC3T3 cells were seeded on composite scaffolds with different pearl concentration. The MTT assay revealed that the cell proliferation of MC3T3 was accelerated during the incubation from 1 day to 6 days. Under the same conditions, the scaffolds containing pearl powders showed higher OD values than pristine PHBV did as shown in Fig. 11. In Fig. 12, the PHBV after mineralization showed a better biocompatibility than pristine PHBV. This indicated that HA also could improve biocompatibility of the scaffold.

The morphology of MC3T3 cells seeded on different samples was observed by confoeal laser scanning microscopy after cultured for 3 days. In Fig. 13, the cell nucleus and cytoplasm of MC3T3 cells growing on the various PHBV nanofiber scaffolds with different pearl powder and HA contents were spindle-shaped, the cells were attached to the scaffold and the pseudopods stretched out. The results suggest that the electrospun PHBV/pearl nanofiber can provide a good culture condition for cells.

4. Conclusion

In this work, we successfully fabricated PHBV/pearl composite nanofiber scaffolds. The incorporation of pearl powder is in favor of spinning of PHBV. Mineralization ability of these composite nanofiber scaffolds was greatly enhanced due to naturally non-toxic pearl powder, which act as crystal nucleus for HA particle depositing. The weight increase of HA on scaffolds is proportional to the content of pearl powder. The introduction of pearl powder can also improve the cell activity of PHBV nanofiber and promote the cells proliferation, which will in turn contribute to the biocompatibility of PHBV nanofiber scaffold. Therefore, the prepared PHBV/pearl composite nanofiber scaffolds would be a promising candidate as an osteoconductive composite material for bone repairing.

References

[1] R. Murugan, S. Ramakrishna, Compos. Sci. Technol. 65 (15) (2005) 2385–2406.
[2] I.O. Smith, X.H. Liu, L.A. Smith, et al., Wiley Interdiscip. Rev.: Nanomed. Nanobiotechnol. 1 (2) (2009) 226–236.
[3] T.J. Sill, H.A. von Recum, Biomaterials 29 (13) (2008) 1989–2006.
[4] S. Agarwal, J.H. Wendorff, A. Greiner, Polymer 49 (26) (2008) 5603–5621.
[5] J.H. Jang, O. Castano, H.W. Kim, Adv. Drug Deliv. Rev. 61 (12) (2009) 1065–1083.
[6] Q.P. Pham, U. Sharma, A.G. Mikos, Tissue Eng. 12 (5) (2006) 1197–1211.
[7] S. Chakraborty, I. Liao, A. Adler, et al., Adv. Drug Deliv. Rev. 61 (12) (2009) 1043–1054.
[8] D. Li, Y. Xia, Adv. Mater. 16 (14) (2004) 1151–1170.
[9] J. Zeng, X. Xu, X. Chen, et al., J. Control. Release 92 (3) (2003) 227–231.
[10] H. Yoshimoto, Y.M. Shin, H. Terai, et al., Biomaterials 24 (12) (2003) 2077–2082.
[11] J. Yuan, Z.C. Xing, S.W. Park, et al., Macromol. Res. 17 (11) (2009) 850–855.
[12] W. Meng, Z.C. Xing, K.H. Jung, et al., J. Mater. Sci.: Mater. Med. 19 (8) (2008) 2799–2807.
[13] E.I. Paşcu, J. Stokes, G.B. McGuinness, Mater. Sci. Eng.: C 33 (8) (2013) 4905–4916.

[14] A. Suslu, A.Z. Albayrak, A.S. Urkmez, et al., J. Mater. Sci.: Mater. Med. 25 (12) (2014) 2677–2689.
[15] N. Sultana, T.H. Khan, J. Nanomater. 2012 (2012) 1.
[16] N. Sultana, M. Wang, Biofabrication 4 (1) (2012) 015003.
[17] A. Ndreu, L. Nikkola, H. Ylikauppila, et al., Nanomedicine (2008) (http://www.futuremedicine.com/loi/nnm).
[18] S.M. Cool, B. Kenny, A. Wu, et al., J. Biomed. Mater. Res. Part A 82 (3) (2007) 599–610.
[19] J. Xie, X. Li, Y. Xia, Macromol. Rapid Commun. 29 (22) (2008) 1775–1792.
[20] J.H. Song, H.E. Kim, H.W. Kim, J. Mater. Sci.: Mater. Med. 19 (8) (2008) 2925–2932.
[21] G. Sui, X. Yang, F. Mei, et al., J. Biomed. Mater. Res. Part A 82 (2) (2007) 445–454.
[22] A. Flausse, C. Henrionnet, M. Dossot, et al., J. Biomed. Mater. Res. Part A 101 (11) (2013) 3211–3218.
[23] Y. Shen, J. Zhu, H. Zhang, et al., Biomaterials 27 (2) (2006) 281–287.
[24] Y.L. Yang, C.H. Chang, C.C. Huang, et al., Bio-med. Mater. Eng. 24 (1) (2014) 979–985.
[25] T. Kokubo, H. Takadama, Biomaterials 27 (15) (2006) 2907–2915.
[26] K. Rezwan, Q.Z. Chen, J.J. Blaker, et al., Biomaterials 27 (18) (2006) 3413–3431.
[27] I. Armentano, M. Dottori, E. Fortunati, et al., Polym. Degrad. Stab. 95 (11) (2010) 2126–2146.
[28] C.Q. Ning, Y. Zhou, Biomaterials 23 (14) (2002) 29.